*American Mineralogist, Volume 91, pages 526–532, 2006*

# Parvo-mangano-edenite, parvo-manganotremolite, and the solid solution between Ca and $Mn^{2+}$ at the M4 site in amphiboles

**Roberta Oberti,[1,*] Fernando Cámara,[1] Giancarlo Della Ventura,[2] Gianluca Iezzi,[3] and Alan I. Benimoff[4]**

[1]CNR-Istituto di Geoscienze e Georisorse, Unità di Pavia, via Ferrata 1, I-27100 Pavia, Italy
[2]Dipartimento di Scienze Geologiche, Università di Roma Tre, largo S. L. Murialdo 1, I-00146 Roma, Italy
[3]Dipartimento di Scienze della Terra, Università G. D'Annunzio, I-66013 Chieti Scalo, Italy
[4]Department of Engineering Science and Physics, College of Staten Island, New York 10314-0000, U.S.A.

## Abstract

This work reports the crystal-chemical characterization of Mn-rich amphiboles from the Grenville Marble of the Arnold mine, Fowler, St. Lawrence Co., New York (U.S.A.), which were previously described by Benimoff et al. (1991) as "manganoan silicic edenite." According to the new nomenclature scheme for monoclinic amphiboles (Leake et al. 2004) the ideal composition of reference, $^{A}Na\ ^{B}(CaMn)\ ^{C}Mg_5\ ^{T}(Si_7Al)O_{22}(OH)_2$ with Ca > 1 apfu, is an end-member of the newly defined Group 5, and is named parvo-mangano-edenite. Re-examination of the original rock specimen showed significant inter- and intra-crystalline compositional variations, which can be expressed by the $^{A}Na_{-1}\ ^{T}Al_{-1}\ ^{A}\square_1\ ^{T}Si_1$ and $^{B}Mn_2\ ^{B}Ca_{-2}$ exchange vectors. The first vector leads to parvo-manganotremolite, ideally $^{A}\square\ ^{B}(CaMn)\ ^{C}Mg_5\ ^{T}Si_8O_{22}(OH)_2$ with Ca > 1. The second mechanism was never found to reach Mn dominance; however, crystal-chemical analysis does not provide any evidence of structural limits, and thus the magno-calcic counterparts of the Group 5 amphiboles of this work may occur in similar but Mn-richer genetic environments. The presence of Mn at the B site helps to stabilize the charge arrangement of edenite.

The parvo-mangano-edenite crystal with composition closest to the end-member, i.e., $^{A}(Na_{0.74}K_{0.02})\ ^{B}(Ca_{1.27}Mn_{0.73})\ ^{C}(Mg_{4.51}Mn^{2+}_{0.28}Fe^{2+}_{0.05}Fe^{3+}_{0.03}Al_{0.12}Ti_{0.01})\ ^{T}(Si_{7.07}Al_{0.93})O_{22}(OH)_2$, has $a$ = 9.8260(5), $b$ = 18.0487(9), $c$ = 5.2840(4) Å, β = 104.55(1)°, $V$ = 907.1 Å$^3$ ($Z$ = 2); the calculated density is 3.11 g/cm$^3$. The parvo-mangano tremolite crystal, with composition $^{A}(Na_{0.44}K_{0.01})\ ^{B}(Ca_{1.13}Mn_{0.83}Na_{0.04})\ ^{C}(Mg_{4.69}Mn^{2+}_{0.21}Fe^{2+}_{0.03}Fe^{3+}_{0.01}Al_{0.06})\ ^{T}(Si_{7.52}Al_{0.48})O_{22}\ (OH)_2$, has $a$ = 9.7807(5), $b$ = 18.0548(9), $c$ = 5.2928(4) Å, β = 104.19(1)°, $V$ = 906.1 Å$^3$ ($Z$ = 2); the calculated density is 3.08 g/cm$^3$. The different compositions are virtually indistinguishable under the optical microscope, but can be identified by a measure of their unit-cell parameters. The single-crystal FTIR spectrum of parvo-mangano-edenite in the OH-stretching region shows two main absorptions at 3711 and 3671 cm$^{-1}$, plus shoulders at 3695, 3660, and 3641 cm$^{-1}$, respectively. FTIR spectroscopy indicates extensive short-range-order of cations in these amphiboles.

**Keywords:** Analysis, chemical (mineral), amphiboles, crystal structure, parvo-mangano-edenite, parvo-manganotremolite, IR spectroscopy, new minerals

## Introduction and nomenclature

A revision of the amphibole nomenclature has been recently approved by the Amphibole Subcommitte of the IMA-CNMMN (Leake et al. 2004). The main novelty of this report is the definition of a new Group 5 for monoclinic amphiboles, which is intermediate between $^{B}$(Mg, Fe, Mn, Li) amphiboles (Group 1) and $^{B}$(Ca, Na) amphiboles (Groups 2–4). The compositional limits defining this new group are 0.50 < $^{B}$(Mg, Fe, Mn, Li) < 1.50 and 0.50 ≤ $^{B}$(Ca, Na) ≤ 1.50 atoms per formula unit (apfu). Group 5 amphiboles with $^{B}$Li > 0.50 apfu generally belong to the continuous solid-solution defined by the exchange vector $^{B}Na_2\ ^{B}Li_{-2}$, and the intermediate compositions with $^{B}(Na_1Li_1)$ deserve new root names [e.g., ferri-ottoliniite: $^{A}\square\ ^{B}(Na_1Li_1)\ ^{C}(Mg_3Fe^{3+}_2)Si_8O_{22}(OH)_2$ and ferriwhittakerite: $^{A}Na\ ^{B}(NaLi)\ ^{C}(Mg_2Fe^{3+}_2Li)Si_8O_{22}(OH)_2$; Oberti et al. 2004]. In contrast, Group 5 amphiboles with $^{B}$Li ≤ 0.50 apfu maintain the root name pertinent to the relevant charge arrangement and the main B-site cation, with a further prefix to indicate whether solid-solution occurs with a smaller (parvo-) or a larger (magno-) cation. Further prefixes denoting homovalent substitutions are added according to the usual rules (Leake et al. 1997, 2004).

Group 5 amphiboles are particularly interesting because they allow investigation of the solid solution between small (Li, Mg, $Fe^{2+}$, $Mn^{2+}$) and large (Na, Ca) cations at the B sites. These cations are known to have distinct coordination numbers [namely, sixfold, (6+2)-fold, and eightfold in $C2/m$ symmetry] and geometries, a feature that generally implies two distinct crystallographic subsites (M4 and M4') in the refinement of solid-solution terms.

Only two examples of Group 5 amphiboles with $^{B}$Li ≤ 0.5 apfu are known in nature. The first is the composition $^{A}(Na_{0.30}K_{0.03})\ ^{B}(Na_{0.87}Ca_{0.39}Mn_{0.57}Mg_{0.17})\ ^{C}(Mg_{3.84}Mn^{2+}_{0.38}Fe^{3+}_{0.72}Li_{0.06})\ ^{T}(Si_{7.88}Al_{0.12})O_{22}\ (OH_{1.60}F_{0.40})$, described by Oberti and Ghose (1993), which

* E-mail: oberti@crystal.unipv.it

must now be named parvowinchite (IMA-CNMMN 2003-066), ideally $^{A}\square^{B}(NaMn)^{C}(Mg_4Fe^{3+})^{T}Si_8O_{22}(OH)_2$. The second example is given by some amphibole compositions, which can be referred to the ideal end-member $^{A}Na^{B}(CaMn)^{C}Mg_5{}^{T}(Si_7Al)O_{22}(OH)_2$ with Ca > 1 apfu, first described by Benimoff et al. (1991) as "manganoan silicic edenites." These compositions are now recognized with the new name parvo-mangano-edenite (IMA-CNMMN 2003-062). We have characterized this amphibole using microchemical analysis, structure refinement, and FTIR analysis. During this work, compositions referable to parvo-manganotremolite, ideally $^{A}\square^{B}(CaMn)^{C}Mg_5{}^{T}Si_8O_{22}(OH)_2$, were first found at the rims of parvo-mangano-edenite crystals, and then as a fairly homogeneous crystal (sequence number 1104 in the CNR-IGG-PV database), which was thus recognized as the holotype specimen (IMA-CNMMN 2004-045). Here, we give a formal description and crystal-chemical interpretation of these two new species.

The charge arrangement of parvo-mangano-edenite is the same as that of edenite. However, edenite [$^{A}Na^{B}Ca_2{}^{C}Mg_5{}^{T}(Si_7Al)O_{22}(OH)_2$] has never been found either in nature or in synthetic products (Boschmann et al. 1994 and references therein), whereas its ferro- and fluoro-counterparts are known to be stable (Graham and Navrotsky 1986; Deer et al. 1997; Gianfagna and Oberti 2001). For this reason, investigation of the substitution of $^{B}Ca^{2+}$ ($^{[8]}r$ = 1.12 Å) with $Mn^{2+}$ ($^{[8]}r$ = 0.96 Å) may also contribute to our understanding of the structural constraints which hinder the stability of edenite.

## Occurrence and description of the sample

Parvo-mangano-edenite and parvo-manganotremolite occur in a manganiferous pod in the Grenville marble of the Arnold open pit, which is operated by the Governeur Talc Company as a source of industrial talc (talc-tremolite). The Arnold mine is near Fowler, St. Lawrence Co., New York, U.S.A. (44°16' N, 75°23' W). The manganiferous pod in the Arnold pit consists of stratified rocks in which layers 0.5 to 3.5 mm thick, containing mostly polycrystalline braunite, alternate with pale pinkish-brown layers composed mostly of calciferous Mn-rich amphibole with minor garnet ($Sp_{81.8}Py_{8.8}Gr_{8.1}Al_{1.3}$) and talc. Details of the geology of the outcrop are given in Benimoff et al. (1991). The peak conditions to which the Grenville Marble sequence was subjected during regional metamorphism are estimated to be 625 ± 25 °C (calcite-dolomite geothermometry) and 6.5 ± 0.5 kbar (sphalerite-pyrite-pyrrhotite geobarometry) (Brown et al. 1987). Parvo-manganotremolite often occurs at the rims of parvo-mangano-edenite; therefore, it is assumed to crystallize during later stages.

The analyzed single-crystals and crystal concentrates from the same rock specimen have been deposited at the Museo di Mineralogia, Dipartimento di Scienze della Terra, Università degli Studi di Pavia, under the numbers 2003-01 (parvo-mangano-edenite) and 2004-02 (parvo-manganotremolite). A rock sample has also been deposited at the Smithsonian Institute, Washington D.C., under the numbers 174043 (parvo-mangano-edenite) and 174043AO (parvo-manganotremolite).

## Appearance and physical properties

Parvo-mangano-edenite and parvo-manganotremolite cannot be easily distinguished under the optical microscope, and were first identified by their unit-cell parameters. They both have a very pale, pinkish brown color in thick crushed grains, and a vitreous luster. They show no fluorescence under long- and short-wave ultraviolet light, are brittle with uneven fracture, and show the characteristic {110} cleavage of monoclinic amphiboles. The crystals are prismatic, elongated on [001]; the grain size is typically 0.2–0.5 mm. The density measured from a 200 mg crystal separate hand picked from the rock and containing ~10% braunite in the form of disseminate minute inclusions is 3.28 g/cm$^3$ (Benimoff et al. 1991); the density calculated based on the present work is 3.11 g/cm$^3$ for parvo-mangano-edenite (crystal 1103) and 3.08 g/cm$^3$ for parvo-manganotremolite (crystal 1104).

Optical properties were determined by Benimoff et al. (1991), using the immersion method and white light. Refraction indexes are $\alpha$ = 1.620(2), $\beta$ = 1.632(2), $\gamma$ = 1.642(2); 2*V* (calc.) = 84°. When using the average *n* value of 1.6313, the crystal-chemical formulae and the calculate density values, the compatibility (1-$K_P/K_C$) index is 0.011 (superior) for parvo-mangano tremolite and 0.016 (superior) for parvo-mangano-edenite. This confirms that optical measurements are not useful for distinguishing these two species. Parvo-mangano-edenite and parvo-manganotremolite are weakly pleochroic, with *Z* = pale pinkish brown, *Y* = pale orange brown, and *X* = colorless; *Z* ^ **c** = 33°.

## X-ray analysis and structure refinement

Crystals were selected based on optical and diffraction properties. X-ray analysis and data collection were done with a Philips PW-1100 four-circle diffractometer using graphite-monochromatized Mo*K*$\alpha$ X-radiation. Unit-cell dimensions were calculated from least-squares refinement of the *d*-values obtained from 50 rows of the reciprocal lattice by measuring the centroid of gravity of each reflection and of the corresponding antireflection in the range $-30 < \theta < 30°$. A full-matrix unweighted least-squares refinement on *F* was done using a program specifically written at the CNR-IGG-PV to deal with complex solid solution terms (Cannillo, personal communication).

Three crystals out of the many characterized during this work were selected as the most representative for this paper. Crystal 1103 (0.50 × 0.25 × 0.20 mm) is the one closest to nominal parvo-mangano-edenite, crystal 1104 (0.34 × 0.16 × 0.13 mm) is within the compositional field of parvo-manganotremolite, crystal 1079 (0.49 × 0.33 × 0.18 mm) is zoned, with the core referable to parvo-mangano-edenite and the rim to parvo-manganotremolite. Table 1 lists selected crystal and refinement data, Table 2 lists atom coordinates, equivalent isotropic displacement parameters (Å$^2$), and refined site-scattering values (ss, epfu), and Table 3 lists the geometric parameters relevant for the description of the crystal structure. Tables 4 and 5[1] give observed and calculated structure factors and the anisotropic components of the atomic displacement parameters.

Due to the large intra- and inter-crystalline compositional variations, the Cu*K*$\alpha$ X-ray powder diffraction patterns requested for the description of a new mineral were calculated from the single-crystal data, and are reported in Table 6.

## Microchemical data

The simplified formula of parvo-mangano-edenite, $^{A}Na^{B}(Ca_1Mn_1)^{C}Mg_5{}^{T}(Si_7Al)O_{22}(OH)_2$, requires: $Na_2O$ 3.65, MgO 23.73, CaO 6.60, MnO 8.35, $Al_2O_3$ 6.00, $SiO_2$ 49.55, $H_2O$ 2.12; total

[1] Deposit item AM-06-014, Tables 4 and 5. Deposit items are available two ways: For a paper copy contact the Business Office of the Mineralogical Society of America (see inside front cover of recent issue) for price information. For an electronic copy visit the MSA web site at http://www.minsocam.org, go to the American Mineralogist Contents, find the table of contents for the specific volume/issue wanted, and then click on the deposit link there.

**TABLE 1.** Sample codes and selected crystal and refinement data for the crystals of this work

| End-member of reference | SEQ | *a* (Å) | *b* (Å) | *c* (Å) | β (°) | *V* (Å³) | $R_{sym}$ % | $R_{all}$ % | $R_{obs}$% | no. $F_{all}$ | no. $F_{obs}$ |
|---|---|---|---|---|---|---|---|---|---|---|---|
| parvo-mangano-edenite | 1103 | 9.8260(5) | 18.0487(9) | 5.2840(4) | 104.55(1) | 907.1 | 3.5 | 2.8 | 2.2 | 1379 | 1196 |
| parvo-manganotremolite | 1104 | 9.7807(5) | 18.0548(9) | 5.2928(4) | 104.19(1) | 906.1 | 3.4 | 3.7 | 2.2 | 1376 | 1058 |
| parvo-mangano-edenite | 1079 | 9.795(3) | 18.047(6) | 5.2869(3) | 104.28(3) | 905.7 | 1.6 | 3.2 | 2.8 | 1376 | 1244 |

*Notes:* SEQ is the sequence number in the CNR-IGG-PV amphibole database; *R* are the standard disagreement indices calculated for the corrected intensities of equivalent monoclinic reflections ($R_{sym}$), and for the observed and calculated structure factors (*F*) of all the reflections ($R_{all}$) and of those used for the refinement ($I > 3\sigma_I$, $R_{obs}$).

**TABLE 2.** Atom coordinates, refined site-scattering values (ss, epfu), and equivalent atom displacement parameters ($B_{eq}$, Å²)

| Atom | ss | *x* | *y* | *z* | $B_{eq}$ | Atom | ss | *x* | *y* | *z* | $B_{eq}$ | Atom | ss | *x* | *y* | *z* | $B_{eq}$ |
|---|---|---|---|---|---|---|---|---|---|---|---|---|---|---|---|---|---|
| parvo-mangano-edenite (1103) | | | | | | parvo-manganotremolite (1104) | | | | | | parvo-mangano-edenite (zoned, 1079) | | | | | |
| O1 | | 0.1105(1) | 0.0860(1) | 0.2175(3) | 0.63 | O1 | | 0.1115(2) | 0.0859(1) | 0.2165(3) | 0.64 | O1 | | 0.1111(2) | 0.0860(1) | 0.2175(3) | 0.68 |
| O2 | | 0.1206(1) | 0.1723(1) | 0.7252(3) | 0.64 | O2 | | 0.1204(2) | 0.1720(1) | 0.7239(3) | 0.69 | O2 | | 0.1209(2) | 0.1722(1) | 0.7248(3) | 0.70 |
| O3 | | 0.1091(2) | 0 | 0.7156(4) | 0.67 | O3 | | 0.1103(2) | 0 | 0.7147(4) | 0.65 | O3 | | 0.1097(2) | 0 | 0.7146(4) | 0.71 |
| O4 | | 0.3688(2) | 0.2478(1) | 0.7827(3) | 0.99 | O4 | | 0.3691(2) | 0.2477(1) | 0.7830(3) | 1.03 | O4 | | 0.3692(2) | 0.2476(1) | 0.7824(3) | 1.04 |
| O5 | | 0.3483(2) | 0.1369(1) | 0.1000(3) | 1.03 | O5 | | 0.3482(2) | 0.1349(1) | 0.0930(3) | 0.99 | O5 | | 0.3485(2) | 0.1356(1) | 0.0952(3) | 1.12 |
| O6 | | 0.3449(2) | 0.1153(1) | 0.5967(3) | 1.08 | O6 | | 0.3455(2) | 0.1169(1) | 0.5880(3) | 1.02 | O6 | | 0.3454(2) | 0.1161(1) | 0.5919(3) | 1.15 |
| O7 | | 0.3410(3) | 0 | 0.2749(5) | 1.06 | O7 | | 0.3407(3) | 0 | 0.2783(5) | 1.02 | O7 | | 0.3411(3) | 0 | 0.2767(5) | 1.09 |
| T1 | | 0.2815(1) | 0.0845(1) | 0.2960(1) | 0.50 | T1 | | 0.2822(1) | 0.0843(1) | 0.2923(1) | 0.50 | T1 | | 0.2819(1) | 0.0844(1) | 0.2938(1) | 0.53 |
| T2 | | 0.2911(1) | 0.1713(1) | 0.8032(1) | 0.51 | T2 | | 0.2913(1) | 0.1710(1) | 0.7995(1) | 0.55 | T2 | | 0.2914(1) | 0.1711(1) | 0.8008(1) | 0.58 |
| M1 | 25.8 | 0 | 0.0880(1) | ½ | 0.53 | M1 | 25.6 | 0 | 0.0878(1) | ½ | 0.59 | M1 | 25.7 | 0 | 0.0879(1) | ½ | 0.66 |
| M2 | 27.3 | 0 | 0.1766(1) | 0 | 0.55 | M2 | 26.5 | 0 | 0.1767(1) | 0 | 0.62 | M2 | 26.4 | 0 | 0.1767(1) | 0 | 0.59 |
| M3 | 12.5 | 0 | 0 | 0 | 0.55 | M3 | 12.5 | 0 | 0 | 0 | 0.63 | M3 | 12.5 | 0 | 0 | 0 | 0.63 |
| M4 | 42.1 | 0 | 0.2736(1) | ½ | 1.32 | M4 | 44.2 | 0 | 0.2713(1) | ½ | 1.42 | M4 | 41.1 | 0 | 0.2726(1) | ½ | 1.39 |
| M4′ | 2.1 | 0 | 0.2524(6) | ½ | 1.01 | M4′ | | | | | | M4′ | 4.3 | 0 | 0.2583(3) | ½ | 1.22 |
| A | 1.0 | 0 | ½ | 0 | 0.89 | A | 0.6 | 0 | ½ | 0 | 1.92 | A | 0.7 | 0 | ½ | 0 | 1.05 |
| A*m* | 2.8 | 0.043(1) | ½ | 0.103(2) | 2.49 | A*m* | 2.4 | 0.043(2) | ½ | 0.106(4) | 3.37 | A*m* | 2.9 | 0.045(2) | ½ | 0.108(3) | 3.26 |
| A2 | 3.7 | 0 | 0.4724(5) | 0 | 2.54 | A2 | 2.0 | 0 | 0.4714(9) | 0 | 2.32 | A2 | 3.0 | 0 | 0.4731(7) | 0 | 3.17 |
| H | | 0.188(6) | 0 | 0.759(9) | 1.36 | H | | 0.204(8) | 0 | 0.768(15) | 2.06 | H | | 0.203(5) | 0 | 0.767(9) | 1.01 |

**TABLE 3.** Selected refinement results [bond lengths (Å), interatomic distances (Å), and interatomic angles (°)]

| | 1103 | 1104 | 1079 | | 1103 | 1104 | 1079 | | 1103 | 1104 | 1079 |
|---|---|---|---|---|---|---|---|---|---|---|---|
| T1-O1 | 1.627(1) | 1.619(2) | 1.622(2) | M1-O1 ×2 | 2.055(1) | 2.060(2) | 2.054(2) | M4′-O2 ×2 | 2.050(1) | | 2.130(2) |
| T1-O5 | 1.655(1) | 1.643(2) | 1.649(2) | M1-O2 ×2 | 2.104(1) | 2.102(2) | 2.106(2) | M4′-O4 ×2 | 2.205(2) | | 2.197(2) |
| T1-O6 | 1.651(2) | 1.644(2) | 1.648(2) | M1-O3 ×2 | 2.087(1) | 2.090(2) | 2.087(2) | M4′-O5 ×2 | 3.016(2) | | 2.980(2) |
| T1-O7 | 1.647 (1) | 1.634(2) | 1.640(1) | <M1-O> | 2.082 | 2.084 | 2.082 | M4′-O6 ×2 | 2.946(2) | | 2.834(2) |
| <T1-O> | 1.645 | 1.635 | 1.640 | OAV | 36.54 | 35.07 | 35.15 | [8]<M4′-O> | 2.554 | | 2.535 |
| TAV | 5.23 | 4.34 | 5.05 | OQE | 1.0112 | 1.0107 | 1.0108 | | | | |
| TQE | 1.0012 | 1.0010 | 1.0012 | M2-O1 ×2 | 2.132(2) | 2.139(2) | 2.137(2) | A-O5 ×4 | 3.000(2) | 2.956(2) | 2.969(2) |
| | | | | M2-O2 ×2 | 2.094(1) | 2.091(2) | 2.092(2) | A-O6 ×4 | 3.092(2) | 3.143(2) | 3.119(2) |
| T2-O2 | 1.622(1) | 1.621(2) | 1.619(2) | M2-O4 ×2 | 2.025(2) | 2.025(2) | 2.026(2) | A-O7 ×2 | 2.386(2) | 2.392(2) | 2.384(3) |
| T2-O4 | 1.595(2) | 1.593(2) | 1.592(2) | <M2-O> | 2.084 | 2.085 | 2.085 | [10]<A-O> | 2.914 | 2.918 | 2.912 |
| T2-O5 | 1.649(2) | 1.650(2) | 1.648(2) | OAV | 21.31 | 21.54 | 21.09 | | | | |
| T2-O6 | 1.668(2) | 1.667(2) | 1.665(2) | OQE | 1.0068 | 1.0069 | 1.0067 | A*m*-O5 ×2 | 3.123(2) | 3.083(11) | 3.104(2) |
| <T2-O> | 1.633 | 1.633 | 1.631 | M3-O1 ×4 | 2.069(1) | 2.072(2) | 2.073(2) | A*m*-O5 ×2 | 2.995(2) | 2.954(9) | 2.964(2) |
| TAV | 17.91 | 18.53 | 18.25 | M3-O3 ×2 | 2.054(2) | 2.060(2) | 2.057(2) | A*m*-O6 ×2 | 2.680(2) | 2.721(13) | 2.687(2) |
| TQE | 1.0044 | 1.0046 | 1.0045 | <M3-O> | 2.064 | 2.068 | 2.068 | A*m*-O7 | 2.381(2) | 2.373(16) | 2.380(3) |
| | | | | OAV | 47.26 | 44.30 | 46.10 | A*m*-O7 | 2.536(2) | 2.562(17) | 2.550(3) |
| T1-T1 | 3.050(1) | 3.044(1) | 3.046(2) | OQE | 1.0146 | 1.0136 | 1.0142 | A*m*-O7 | 3.197(2) | 3.177(21) | 3.168(3) |
| T1-T2 | 3.085(1) | 3.090(1) | 3.085(1) | | | | | [9]<A*m*-O> | 2.857 | 2.847 | 2.845 |
| T1-T2 | 3.061(1) | 3.062(1) | 3.061(1) | M4-O2 ×2 | 2.336(2) | 2.307(2) | 2.325(2) | | | | |
| | | | | M4-O4 ×2 | 2.238(2) | 2.223(2) | 2.224(2) | A2-O5 ×2 | 2.606(2) | 2.547(2) | 2.583(2) |
| H-O3 | 0.751(2) | 0.890(2) | 0.887(2) | M4-O5 ×2 | 2.778(2) | 2.854(2) | 2.821(2) | A2-O6 ×2 | 2.782(2) | 2.822(2) | 2.816(2) |
| O6-O7-O6 | 101.80 | 104.70 | 103.34 | M4-O6 ×2 | 2.645(2) | 2.631(2) | 2.632(2) | A2-O7 ×2 | 2.437(2) | 2.447(2) | 2.433(3) |
| O5-O6-O5 | 163.16 | 165.95 | 164.78 | [8]<M4-O> | 2.499 | 2.504 | 2.501 | <A2-O> | 2.608 | 2.606 | 2.611 |

*Note*: Polyhedral angular variance (TAV, OAV) and quadratic elongation (TQE, OQE) as defined by Robinson et al. (1971).

100.00 wt%. The simplified formula of parvo-manganotremolite, $^{A}\square^{B}(Ca_1Mn_1)^{C}Mg_5{}^{T}Si_8O_{22}(OH)_2$, requires: MgO 24.36, CaO 6.78, MnO 8.58, $SiO_2$ 58.11, $H_2O$ 2.18; total 100.00 wt%.

Electron microprobe analysis was done with the same crystals as used for the structure refinement. The operating conditions were: 15 kV, 10 nA, 2 μm beam diameter. The minerals used as standards for *K*α X-ray lines were: Si and Na: albite (TAP); Al: spinel (TAP); Fe: andradite (LiF); Mn: $MnTiO_3$ (LiF); Mg: enstatite (TAP); Ti: $MnTiO_3$ (PET); Cr: pure metal (LiF); Ca: andradite (PET); and K: orthoclase (PET). Given the widespread compositional zoning, many points (38 and 42 points for crystals 1103 and 1104, respectively) were analyzed for each crystal. The water content was calculated to give 2.0 OH groups in the unit formula, as indicated by the structure refinement. The results are reported in Table 7.

Unit formulae were normalized to 24 O atoms and site-populations and oxidation state for Mn and Fe were calculated based on refined site-scattering values and mean bond-lengths (Table 7). In the zoned crystal no. 3, the composition of the volumetrically dominant core corresponds to parvo-mangano-edenite, whereas the composition of the rim corresponds to parvo-manganotremolite.

## FTIR SPECTROSCOPY

A single-crystal unpolarized spectrum was collected at room-*T* in the principal OH-stretching region from a randomly oriented

**TABLE 6.** Calculated Cu*K*α (λ = 1.5418 Å) powder diffraction patterns for parvo-mangano-edenite and parvo-manganotremolite (reflections with $I/I_0 \geq 10$)

| I | 2θ | $d_{calc}$ | h k l | I | 2θ | $d_{calc}$ | h k l | I | 2θ | $d_{calc}$ | h k l | I | 2θ | $d_{calc}$ | h k l |
|---|---|---|---|---|---|---|---|---|---|---|---|---|---|---|---|
| parvo-mangano-edenite (1103) | | | | | | | | | | parvo-manganotremolite (1104) | | | | | |
| 51 | 9.80 | 9.024 | 0 2 0 | 20 | 39.20 | 2.298 | $\bar{1}$ 7 1 | 54 | 9.80 | 9.027 | 0 2 0 | 20 | 39.20 | 2.298 | $\bar{1}$ 7 1 |
| 63 | 10.51 | 8.414 | $\bar{1}$ 1 0 | 17 | 39.65 | 2.273 | 3 1 2 | 62 | 10.54 | 8.395 | $\bar{1}$ 1 0 | 18 | 39.76 | 2.267 | 3 1 2 |
| 19 | 18.19 | 4.878 | 1 1 1 | 45 | 41.75 | 2.164 | 2 6 1 | 23 | 18.20 | 4.874 | 1 1 1 | 44 | 41.69 | 2.167 | 2 6 1 |
| 18 | 19.67 | 4.512 | 0 4 0 | 21 | 44.23 | 2.048 | 2 0 2 | 18 | 19.67 | 4.514 | 0 4 0 | 24 | 44.06 | 2.055 | 2 0 2 |
| 11 | 21.12 | 4.207 | $\bar{2}$ 2 0 | 17 | 44.91 | 2.018 | $\bar{3}$ 5 1 | 13 | 21.17 | 4.198 | $\bar{2}$ 2 0 | 16 | 44.86 | 2.020 | $\bar{3}$ 5 1 |
| 21 | 22.95 | 3.875 | 1 3 1 | 15 | 45.07 | 2.012 | $\bar{4}$ 0 2 | 25 | 22.96 | 3.874 | 1 3 1 | 13 | 45.27 | 2.003 | $\bar{4}$ 0 2 |
| 67 | 26.32 | 3.386 | 1 3 1 | 12 | 48.84 | 1.865 | 1 9 1 | 62 | 26.25 | 3.395 | 1 3 1 | 12 | 48.83 | 1.865 | 1 9 1 |
| 59 | 27.24 | 3.273 | 2 4 0 | 31 | 55.68 | 1.651 | 4 6 1 | 56 | 27.28 | 3.269 | 2 4 0 | 30 | 55.65 | 1.651 | 4 6 1 |
| 75 | 28.59 | 3.123 | 3 1 0 | 16 | 56.95 | 1.617 | $\bar{1}$ 11 0 | 80 | 28.67 | 3.113 | 3 1 0 | 14 | 56.94 | 1.617 | $\bar{1}$ 11 0 |
| 50 | 30.36 | 2.944 | 2 2 1 | 24 | 58.43 | 1.579 | $\bar{1}$ 5 3 | 51 | 30.29 | 2.950 | 2 2 1 | 24 | 58.31 | 1.582 | $\bar{1}$ 5 3 |
| 18 | 31.91 | 2.805 | $\bar{3}$ 3 0 | 13 | 60.49 | 1.530 | $\bar{6}$ 0 2 | 15 | 31.98 | 2.798 | $\bar{3}$ 3 0 | 11 | 60.84 | 1.523 | $\bar{6}$ 0 2 |
| 31 | 32.83 | 2.728 | $\bar{3}$ 3 1 | 24 | 61.26 | 1.513 | $\bar{2}$ 6 3 | 25 | 32.97 | 2.717 | $\bar{3}$ 3 1 | 22 | 61.22 | 1.514 | $\bar{2}$ 6 3 |
| 100 | 33.08 | 2.708 | 1 5 1 | 16 | 61.67 | 1.504 | $\bar{0}$ 12 0 | 100 | 33.02 | 2.713 | 1 5 1 | 14 | 61.64 | 1.505 | $\bar{0}$ 12 0 |
| 57 | 34.59 | 2.593 | $\bar{0}$ 6 1 | 40 | 64.92 | 1.436 | 6 6 1 | 51 | 34.55 | 2.596 | $\bar{0}$ 6 1 | 37 | 65.19 | 1.431 | 6 6 1 |
| 57 | 35.43 | 2.533 | $\bar{2}$ 0 2 | 13 | 68.69 | 1.366 | $\bar{5}$ 1 2 | 59 | 35.47 | 2.531 | $\bar{2}$ 0 2 | 13 | 68.56 | 1.369 | $\bar{5}$ 1 2 |
| 37 | 38.56 | 2.335 | $\bar{3}$ 5 1 | 15 | 73.18 | 1.293 | $\bar{2}$ 12 2 | 34 | 38.68 | 2.328 | $\bar{3}$ 5 1 | 16 | 73.18 | 1.293 | $\bar{2}$ 12 2 |
| 22 | 38.85 | 2.318 | 4 2 1 | 10 | 80.15 | 1.197 | 5 11 2 | 21 | 39.04 | 2.307 | 4 2 1 | 10 | 80.36 | 1.195 | 5 11 2 |

**TABLE 7.** EMP analyses for the crystals of this work. Unit-formulae calculated on the basis of 24 O atoms per formula unit (pfu)

| | Observed range (wt%) | Oxides (wt%, e.s.d.) | | | | | | Unit formulae (apfu) | | | | |
|---|---|---|---|---|---|---|---|---|---|---|---|---|
| | | 1103 38 pt | 1104 42 pt | 1079 ave 38 pts | 1079 core | 1079 rim | | 1103 | 1104 | 1079 ave | 1079 core | 1079 rim |
| $SiO_2$ | 48.41–54.88 | 49.33(0.73) | 52.46(0.74) | 52.18(1.28) | 51.07(0.25) | 53.71(0.55) | $^{T}$Si | 7.07 | 7.52 | 7.36 | 7.23 | 7.54 |
| $TiO_2$ | | 0.10(0.03) | 0.03(0.02) | 0.10 | 0.10 | 0.10 | $^{T}$Al | 0.93 | 0.48 | 0.64 | 0.77 | 0.46 |
| $Al_2O_3$ | 2.60–6.81 | 6.24(0.48) | 3.21(0.33) | 4.61(1.10) | 5.56(0.28) | 3.30(0.47) | | | | | | |
| FeO | 0.00–0.86 | 0.74(0.09) | 0.32(0.05) | 0.30(0.15) | 0.41(0.06) | 0.13(0.08) | $^{C}$Al | 0.12 | 0.06 | 0.12 | 0.15 | 0.08 |
| MnO | 7.87–11.02 | 8.45(0.19) | 8.50(0.22) | 9.61(0.54) | 9.25(0.26) | 10.17(0.40) | $^{C}$Ti | 0.01 | 0.00 | 0.01 | 0.01 | 0.01 |
| MgO | 20.69–22.68 | 21.14(0.28) | 21.99(0.20) | 21.72(0.45) | 21.35(0.12) | 22.26(0.19) | $^{C}$$Fe^{2+}$ | 0.05 | 0.03 | 0.02 | 0.04 | 0.02 |
| CaO | 5.82–8.57 | 8.30(0.16) | 7.38(0.21) | 7.05(0.54) | 7.47(0.14) | 6.45(0.38) | $^{C}$$Fe^{3+}$ | 0.03 | 0.01 | 0.02 | 0.01 | 0.00 |
| $Na_2O$ | 1.42–2.84 | 2.65(0.16) | 1.73(0.14) | 2.12(0.37) | 2.43(0.08) | 1.68(0.18) | $^{C}$Mg | 4.51 | 4.69 | 4.56 | 4.50 | 4.65 |
| $K_2O$ | 0.02–0.16 | 0.12(0.02) | 0.06(0.02) | 0.08(0.03) | 0.11(0.01) | 0.06(0.02) | $^{C}$Mn | 0.28 | 0.21 | 0.27 | 0.29 | 0.24 |
| $H_2O_{cal}$ | | 2.10 | 2.09 | 2.12 | 2.12 | 2.12 | | | | | | |
| Total | | 99.03 | 97.78 | 99.89 | 99.87 | 100.00 | $^{B}$Mn | 0.73 | 0.83 | 0.88 | 0.82 | 0.97 |
| | | | | | | | $^{B}$Ca | 1.27 | 1.13 | 1.07 | 1.13 | 0.97 |
| Calculated site-scattering values (epfu) | | | | | | | $^{B}$Na | 0.00 | 0.04 | 0.05 | 0.05 | 0.06 |
| A group sites | | 8.56 | 5.04 | 6.02 | 7.2 | 4.59 | | | | | | |
| B group sites | | 43.65 | 43.75 | 43.95 | 43.65 | 44.31 | $^{A}$Na | 0.74 | 0.44 | 0.53 | 0.62 | 0.40 |
| C group sites | | 65.08 | 63.32 | 64.29 | 64.72 | 63.58 | $^{A}$K | 0.02 | 0.01 | 0.01 | 0.02 | 0.01 |
| Total | | 117.28 | 112.11 | 114.26 | 115.57 | 112.48 | | | | | | |
| | | | | | | | $^{X}$OH | 2.00 | 2.00 | 2.00 | 2.00 | 2.00 |

*Note*: The site populations obtained based on refinement results for the M and T-sites are:
1103: $^{M1}(Mg_{1.86}Mn^{2+}_{0.12}Fe^{2+}_{0.02})$ $^{M2}(Mg_{1.79}Mn^{2+}_{0.15}Fe^{3+}_{0.03}Ti^{4+}_{0.01}Al_{0.01}Fe^{2+}_{0.01})$ $^{M3}(Mg_{0.86}Al_{0.11}Fe^{2+}_{0.02}Mn^{2+}_{0.01})$; $^{T1}(Si_{3.07}Al_{0.93})$ $^{T2}Si_4$
1104: $^{M1}(Mg_{1.88}Mn^{2+}_{0.12})$ $^{M2}(Mg_{1.87}Mn^{2+}_{0.09}Fe^{2+}_{0.03}Fe^{3+}_{0.01})$ $^{M3}(Mg_{0.94}Al_{0.06})$ $^{T1}(Si_{3.52}Al_{0.48})$ $^{T2}Si_4$
1079: $^{M1}(Mg_{1.88}Mn^{2+}_{0.11}Fe^{2+}_{0.01})$ $^{M2}(Mg_{1.82}Mn^{2+}_{0.12}Fe^{3+}_{0.02}Al_{0.02}Ti^{4+}_{0.01}Fe^{2+}_{0.01})$ $^{M3}(Mg_{0.86}Al_{0.10}Mn^{2+}_{0.04})$ $^{T1}(Si_{3.36}Al_{0.64})$ $^{T2}Si_4$

fragment, using a NicPlan FTIR microscope equipped with a nitrogen-cooled MCT-A detector and a KBr beamsplitter; the nominal resolution was 4 $cm^{-1}$, and 128 scans were averaged. The spectrum shows (Fig. 1a) two main absorptions at 3711 and 3671 $cm^{-1}$, and a well-defined shoulder at 3695 $cm^{-1}$; two weak shoulders are also resolved at 3660 and 3641 $cm^{-1}$, respectively. This spectrum is virtually identical to the one obtained during a systematic work on amphiboles by Skogby and Rossman (1991) from a crystal (sample number GRR 1619) picked from the same rock as that studied here. These authors identified the sample as "sodian cummingtonite," and did not provide a detailed interpretation of the IR pattern. However, they collected spectra in the α, β, and γ polarizations, and showed that in parvo-mangano-edenite the OH dipole is oriented in the (010) mirror plane, and has maximum absorption along α.

The digitized spectrum of Figure 1a was fitted by interactive optimization followed by least-squares refinement (Della Ventura et al. 1996); the background was treated as linear and all bands were modeled as symmetric Gaussians (Strens 1974). The spectrum was fitted to the smallest number of peaks needed for an accurate description of the profile; the result shows several components, which are labeled from A to H in Figure 1b. On the basis of our previous knowledge of amphiboles (e.g., Della Ventura et al. 1999, 2003; Hawthorne et al. 2000) bands A, B, and C can be assigned to configurations involving an O-H group facing an occupied A-site (Della Ventura 1992; Della Ventura et al. 2003), whereas bands D to H can be assigned to configurations involving the O-H group facing an empty A-site. In particular, the frequency of band A corresponds to that of synthetic richterite (Robert et al. 1989), whose local configuration can be expressed as MgMgMg-OH-$^{A}$Na-SiSi, using the notation M1M1M3-OH-A-T1T2 proposed by Della Ventura et al. (1999). This notation contains all information concerning the NN (nearest-neighbors, left side) and NNN (next-nearest-neighbors, right side) arrangements around the OH group. Band B has the same frequency as the main band in synthetic pargasite, and can thus be assigned to the local configuration MgMgMg-OH-$^{A}$Na-AlSi; its frequency shift with respect to band A (~20 $cm^{-1}$) is due to the presence of Al at the T1 site (Della Ventura et al. 1999). The frequency shift of band C with respect to band B (~20 $cm^{-1}$) is compatible

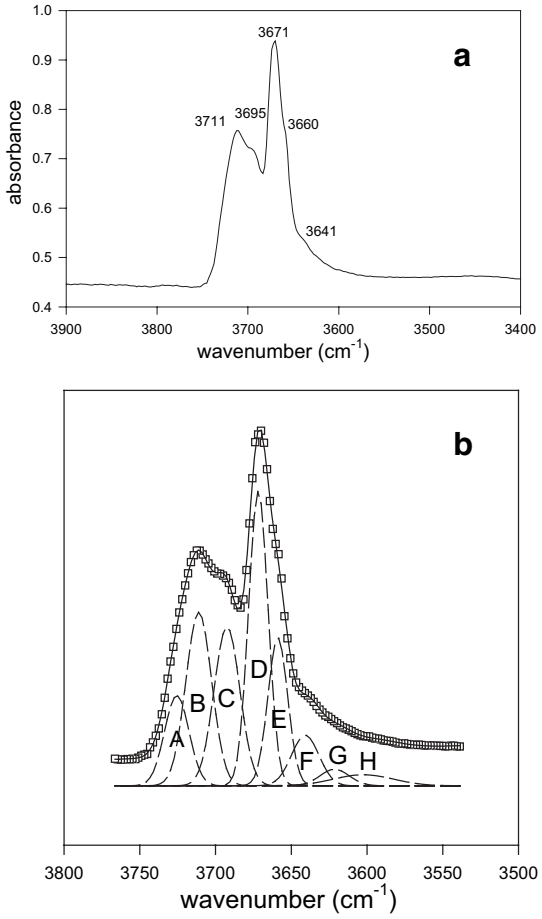


**FIGURE 1.** The FTIR spectrum collected for parvo-mangano-edenite: (**a**) the main absorption frequencies and (**b**) the deconvolution results discussed in the text.

with the presence of a divalent cation different from Mg at the M1 and M3 sites (e.g., Della Ventura et al. 1996); hence, we assign band C to the MgMgMn-OH-$^{A}$Na-AlSi configuration. Band D has the same frequency as tremolite, thus it is assigned to the local configuration MgMgMg-$^{A}\square$-SiSi (Hawthorne et al. 1997). The separations among the quartet of bands D to G are compatible with their assignment to the four local configurations resulting from the distribution of Mg and $Mn^{2+}$ at the M1 and M3 sites (e.g., Della Ventura et al. 1996; Reece et al. 2002). The weak band H is assigned to the local configuration involving a trivalent cation at the M1 or M3 site. Final band assignments are summarized in Table 8. It should be noted that additional components related to the distribution of Mn in local richteritic environments, like MgMgMn-OH-$^{A}$Na-SiSi or MgMnMn-OH-$^{A}$Na-SiSi and MnMnMn-OH-$^{A}$Na-SiSi, could also occur, however such absorptions would completely overlap with bands B, C, and D; these possible features are also included in Table 8. An additional source of uncertainty in the interpretation of the spectrum of Figure 1 is related to the NNN effect of the B-cations (e.g., Iezzi et al. 2004). This effect is however rather weak for the Ca-Mn couple with $\Delta\nu$OH of about 4 $cm^{-1}$ (Papin 2001). Considering these difficulties, and possible variations in absorption coefficients between the different configurations (e.g., Hawthorne et al. 2000) exact quantitative data cannot be extracted from the measured relative band intensities. However, a rough evaluation of the relative amounts of Mg and $Mn^{2+}$ at the M1 and M3 sites done using the procedure discussed in Hawthorne et al. (1996a), and Della Ventura et al. (1996), provides $^{M1,3}$Mg ~2.4 apfu to be compared with 2.72–2.86 apfu from the crystal-chemical formulae in Table 7. This agreement can be considered satisfactory, given the severe band overlapping, suggesting that the proposed band assignment is correct.

**TABLE 8.** Band labels, position ($cm^{-1}$), and assignment for the spectrum of parvo-mangano-edenite

| Band | Wavenumber ($cm^{-1}$) | Configuration |
|---|---|---|
| A | 3725 | $^{A}$Na-MgMgMg-SiSi |
| B | 3711 | $^{A}$Na-MgMgMg-AlSi |
| B* | 3709 | $^{A}$Na-MgMgMn-SiSi |
| C | 3692 | $^{A}$Na-MgMgMn-AlSi |
| C* | 3693 | $^{A}$Na-MgMnMn-SiSi |
| D | 3672 | $^{A}\square$-MgMgMg-SiSi |
| D* | 3677 | $^{A}$Na-MnMnMn-SiSi |
| E | 3659 | $^{A}\square$-MgMgMn-SiSi |
| F | 3641 | $^{A}\square$-MgMnMn-SiSi |
| G | 3621 | $^{A}\square$-MnMnMn-SiSi |
| H | 3603 | $^{A}\square$-MgMgM$^{3+}$-SiSi |

* Values calculated considering a constant negative shift of 16 $cm^{-1}$ for the different (Mg, Mn) configurations at M(1,3) (e.g., Reece et al. 2002)

## CRYSTAL-CHEMISTRY AND CATION ORDERING IN PARVO-MANGANO-EDENITE AND EDENITE

Benimoff et al. (1991) reported analyses of 7 distinct grains from the same rock sample from which holotype parvo-mangano-edenite was extracted. Our point analyses reproduced most of their chemical variations, and can be referred to as parvo-mangano-edenite and parvo-manganotremolite. On the contrary, we could not find confirmatory evidence of their composition no. 2, which would now correspond to a further end-member, to be named "magno-manganocummingtonite" according to Leake et al. (2004).

The exchange vector $^{A}Na_1{}^{T}Al_1{}^{A}\square_{-1}{}^{T}Si_{-1}$, which relates the two end-members described in this paper, also defines the main inter- and intracrystalline compositional differences in the rock sample from Fowler (New York). The additional exchange vector $^{B}Mn_1{}^{B}Ca_{-1}$, which would allow the occurrence of the magno-mangano- counterparts, is also active, albeit in a more restricted range. In particular, compositions with $^{B}Mn > 1$, $^{A}Na > 0.5$, and $^{T}Al > 0.5$ apfu could not be found either in this or in the previous work. This feature is in agreement with the absence (except the orthorhombic end-members sodicgedrite and sodicanthophyllite) of Group 1 amphiboles with a filled A site. A composition of this type with monoclinic symmetry would require a new root name.

Amphiboles having the root-name "edenite" are not common. The $(OH)_2$ compositions reported so far are all enriched in Fe and fall in the compositional field of ferro-edenite, whereas their fluoro- counterparts are enriched in Mg, and fall in the compositional field for fluoro-edenite (Deer et al. 1997; Gianfagna and Oberti 2001).

Hawthorne et al. (1996b) examined the ordering of Na at the A site in amphiboles, and concluded that the preferred local configurations for Ca at the M4 site are $^{M4}$Ca-OH-$^{A2}$Na and $^{M4}$Ca-F-$^{Am}$Na. This model was later supported by the refinement

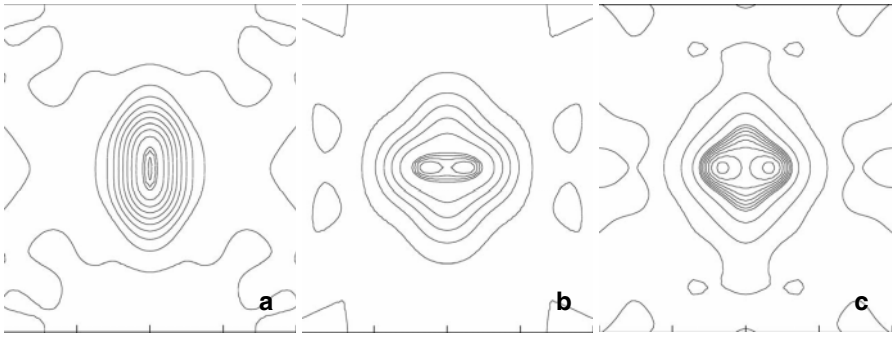


**FIGURE 2.** Difference-Fourier sections at the A-group sites. Sections are approximately parallel to ($\bar{2}$01). The contour intervals are: (**a**) 1 e/Å$^3$ below 10 e/Å$^3$ and 0.2 e/Å$^3$ above 10 e/Å$^3$, (**b**) 1 e/Å$^3$ below 6 e/Å$^3$ and 0.1 e/Å$^3$ above 6 e/Å$^3$, (**c**) 1 e/Å$^3$ below 3.5 e/Å$^3$ and 0.1 e/Å$^3$ above 3.5 e/Å$^3$.

of end-member fluoro-edenite (Gianfagna and Oberti 2001) where $^{A}$Na is indeed totally ordered at A*m* (Figure 2a). In the parvo-mangano-edenite and parvo-manganotremolite crystals of this work, $^{A}$Na distributes between the two sites, with a slight preference for the A2 site in the former crystal, where the Ca content is higher (Table 2 and Figs. 2b and 2c). Because the samples studied here are F-free (Table 7), the occurrence of Na at the A*m* site can be explained by the presence of $Mn^{2+}$ at the B sites which, given its smaller ionic radius, tends to order at a site (M4') closer to the strip of octahedra. This being the case, there is a lower bond-valence contribution incident at the O5 and O6 O atoms, which can be alleviated by having Na at the A*m* position. The same effect was noted in $^{B}$Li amphiboles (Oberti et al. 2003).

Hawthorne (1997) examined the possible ordering schemes for the amphibole end-members using a bond-valence approach. For edenite in particular, he proposed three possible local configurations imposed by the occurrence of Al and Si at the T1 site. The first two are well balanced: $^{M1}Mg^{M2}Mg^{M3}Mg^{B}Ca^{A2}Na^{T1}Al^{T2}Si$ ["edenite(1)"], and $^{M1}Mg^{M2}Mg^{M3}Mg^{B}Ca^{A2}\square^{T1}Si^{T2}Si$ ["edenite(2)"]. The third configuration, $^{M1}Mg^{M2}Mg^{M3}Mg^{B}Ca^{A2}Na^{T1}Si^{T2}Si$ ["edenite(3)"], is equivalent to a tremolite arrangement with additional Na, and thus implies some excess bond-valence contribution incident at the O5 and O6 O atoms which might be accommodated by relaxation of bond lengths. The presence of $Mn^{2+}$ at the M4 site is a further suitable mechanism for reducing bond-valence contributions at O5 and O6. The FTIR spectrum of parvo-mangano-edenite (Fig. 1) confirms this model. The "edenite(1)" configuration is associated with bands B and C (Table 8), and the "edenite(2)" configuration, associated with bands D to G, is the dominant absorption feature, in keeping with the Si excess measured by EMP analysis. The "edenite(3)" configuration is also present, and is associated with band A. The presence of the configurations predicted on bond-valence grounds by Hawthorne (1997) confirms that there is significant short-range order in these structures.

A peculiarity of these compositions is the ordering of the very low amounts of octahedral Al at the M3 site. This assignment is supported by a better agreement between the calculated and refined <M1,2,3-O> values and by the presence of band H in the FTIR spectrum, which also associates $^{M3}$Al with $^{A}\square$. Disorder of Al between the M2 and M3 sites is common only in pargasites close to the nominal composition (Oberti et al. 1995; Della Ventura et al. 1999), where the overall charge arrangement yields an M3 octahedron smaller than in other amphibole compositions.

## REFERENCES CITED

Benimoff, A.I., Benoit, P.H., Moore, P.B., and Sclar, C.B. (1991) A unique manganese-rich silicic edenite in the Grenville marble, Fowler, New York. American Mineralogist, 76, 1431–1433.

Boschmann, K.F., Burns, P.C., Hawthorne, F.C., Raudsepp, M., and Turnock, A.C. (1994) A-site disorder in synthetic fluor-edenite, a crystal-structure study. Canadian Mineralogist, 32, 21–30.

Brown, A.I., Moore, P.B., and Sclar, C.B. (1987) A manganese-rich metamorphic assemblage in the Grenville marble, Balmat, N.Y. Geological Society of America Abstracts with Programs, 19, 5.

Deer, W.A., Howie, R.A., and Zussman, J., eds. (1997) Rock Forming Minerals, Volume 2B: Double-chain Silicates. Second Edition. The Geological Society, London.

Della Ventura, G. (1992) Recent developments in the synthesis and characterization of amphiboles. Synthesis and crystal-chemistry of richterites. Trends in Mineralogy, 1, 153–192.

Della Ventura, G., Robert, J.-L., and Hawthorne, F.C. (1996) Infrared spectroscopy of synthetic (Ni,Mg,Co)-potassium-richterite. Geochimica and Cosmochimica Acta, 5, 55–63.

Della Ventura, G., Hawthorne, F.C., Robert, J.-L., Delbove, F., Welch, M.D., and Raudsepp, M. (1999) Short-range order of cations in synthetic amphiboles along the richterite-pargasite join. European Journal of Mineralogy, 11, 79–94.

Della Ventura, G., Hawthorne, F.C., Robert, J.-L., and Iezzi, G. (2003) Synthesis and infrared spectroscopy of amphiboles along the tremolite-pargasite join. European Journal of Mineralogy, 15, 341–347.

Gianfagna, A. and Oberti, R. (2001) Fluoro-edenite from Biancavilla (Catania, Sicily, Italy): Crystal chemistry of a new amphibole end-member. American Mineralogist, 86, 1489–1493.

Graham, C.M. and Navrotsky, A. (1986) Thermochemistry of the tremolite-edenite amphiboles with applications to amphibole-plagioclase quartzequilibria. Contributions to Mineralogy and Petrology, 93, 18–32.

Hawthorne, F.C. (1997) Short-range order in amphiboles: a bond-valence approach. Canadian Mineralogist, 35, 201–216.

Hawthorne, F.C., Della Ventura, G., and Robert, J.-L. (1996a) Short-range order of (Na,K) and Al in tremolite: an infrared study. American Mineralogist, 81, 782–784.

Hawthorne, F.C., Oberti, R., and Sardone, N. (1996b) Sodium at the A site in clinoamphiboles: The effects of composition on patterns of order. Canadian Mineralogist, 34, 577–593.

Hawthorne, F.C., Della Ventura, G., Robert, J.-L., Welch, M.D., Raudsepp, M., and Jenkins, D.M. (1997) A Rietveld and infrared study of synthetic amphiboles along the potassium-richterite - tremolite join. American Mineralogist, 82, 708–716.

Hawthorne, F.C., Welch, M.D., Della Ventura, G., Shuangxi Liu, Robert, J.-L., and Jenkins, D.M. (2000) Short-range order in synthetic alluminous tremolites: An infrared and triple-quantum MAS NMR study. American Mineralogist, 85, 1716–1724.

Iezzi, G., Cámara, F., Della Ventura, G., Oberti, R., Pedrazzi, G., and Robert, J.-L. (2004) Synthesis, crystal structure and crystal-chemistry of ferriclinoholmquistite, $\square Li_2Mg_3Fe^{3+}{}_2Si_8O_{22}(OH)_2$. Physics and Chemistry of Minerals, 31, 375–385.

Leake, B.E., Woolley, A.R., Arps, C.E.S., Birch, W.D., Gilbert, M.C., Grice, J.D., Hawthorne, F.C., Kato, A., Kisch, H.J., Krivovichev, V.G., Linthout, K., Laird, J., Mandarino, J.A, Maresch, W.V, Nickel, E.H., Rock, N.M.S., Schumacher, J.C., Smith, D.C., Stephenson, N.C.N., Ungaretti, L., Whittaker, E.J.W., and Guo, Y. (1997) Nomenclature of amphiboles: Report of the subcommittee on amphiboles of the International Mineralogical Association, Commission on New Minerals and Mineral Names. American Mineralogist, 82, 1019–1037.

Leake, B.E., Woolley, A.R., Birch, W.D., Burke, E.A.J., Ferraris, G., Grice, J.D., Hawthorne, F.C., Kisch, H.J., Krivovichev, V.G., Schumacher, J.C., Stephenson, N.C.N., and Whittaker, E.J.W. (2004) Nomenclature of amphiboles: additions and revisions to the International Mineralogical Association's amphibole nomenclature. American Mineralogist, 88, 883–887.

Oberti, R. and Ghose, S. (1993) Crystal-chemistry of a complex Mn-bearing alkali amphibole on the verge of exsolution. European Journal of Mineralogy, 5, 1153–1160.

Oberti, R., Hawthorne, F.C., Ungaretti, L., and Cannillo, E. (1995) $^{[6]}$Al disorder in amphiboles from mantle peridotite. Canadian Mineralogist, 33, 867–878.

Oberti, R., Cámara, F., Ottolini, L., and Caballero, J.M. (2003) Lithium in amphiboles: detection, quantification, and incorporation mechanisms in the compositional space bridging sodic and $^{B}$Li amphiboles. European Journal of Mineralogy, 15, 309–319.

Oberti, R., Cámara, F., and Caballero, J.M. (2004) Ferri-ottoliniite and ferriwhittakerite, two new end-members of the new Group 5 for monoclinic amphiboles. American Mineralogist, 88, 888–893.

Papin, A. (2001) Etude Expérimentale et Spectroscopique de la Cristallochimie du Manganèse dans les Silicates Hydroxylés. Unpublished Ph.D. Thesis, University of Orléans, France.

Reece, J.J., Redfern, S.A.T., Welch, M.D., Henderson, C.M.B., and McCammon, C.A. (2002): Temperature-dependent $Fe^{2+}$-$Mn^{2+}$ order-disorder behaviour in amphiboles. Physics and Chemistry of Minerals, 29, 562–570.

Robert, J.L., Della Ventura, G., and Thauvin, J.-L. (1989) The infrared OH-stretching region of synthetic richterites in the system $Na_2O$-$K_2O$-CaO-MgO-$SiO_2$-$H_2O$-HF. European Journal of Mineralogy, 1, 203–211.

Robinson, K., Gibbs, G.V., and Ribbe, P.H. (1971) Quadratic elongation: A quantitative measure of distortion in coordination polyhedra. Science, 172, 567–570.

Skogby, H. and Rossman, G.R. (1991) The intensity of amphibole OH bands in the infrared absorption spectrum. Physics and Chemistry of Minerals, 18, 64–68.

Strens, R.S.J. (1974) The common chain, ribbon and ring silicates. In V.C. Farmer, Ed., The Infrared Spectra of Minerals. Mineralogical Society Monographs, 4, 305–330. Mineralogical Society, London.

MANUSCRIPT RECEIVED FEBRUARY 2, 2005
MANUSCRIPT ACCEPTED BY JULY 9, 2005
MANUSCRIPT HANDLED MARC HIRSCHMANN